

## 21. A TEST OF THE TEMPERATURE, PRESSURE, AND CONDUCTIVITY TOOL AT A GAS-POOR BACKGROUND SITE<sup>1</sup>

William Ussler III,<sup>2</sup> Charles K. Paull,<sup>2</sup> Paul McGill,<sup>2</sup>  
Derryl Schroeder,<sup>3</sup> and Dean Ferrell<sup>3</sup>

### ABSTRACT

A tool to continuously monitor temperature, pressure, and conductivity (TPC) changes during Ocean Drilling Program (ODP) coring was tested at ODP Site 1226. TPC sensors are located on the face of the standard ODP advanced piston corer piston, and the data logging electronics and batteries are embedded within the piston. This tool operates autonomously and requires little shipboard attention. The objective is to monitor the TPC changes that occur in gas-rich and gas hydrate-bearing cores and to learn about the processes that occur during core collection. Gas evolution during core recovery alters the temperature and pressure conditions within the core barrel. By establishing families of ascent curves comprising TPC data from successive cores, variations in the relative amounts of gas and gas hydrates stored in sediments can be determined at individual sites and variations between sites can be assessed. Here, the performance of the TPC tool and the response of the tool at a site without significant quantities of sediment gas are described.

### INTRODUCTION

The temperature, pressure, and conductivity (TPC) tool was developed to measure the effects of expanding gas within the Ocean Drilling Program (ODP) advanced piston corer (APC) assembly during core recovery. In this chapter, we describe the observations that stimulated the

<sup>1</sup>Ussler, W., III, Paull, C.K., McGill, P., Schroeder, D., and Ferrell, D., 2006. A test of the temperature, pressure, and conductivity tool at a gas-poor background site. In Jørgensen, B.B., D'Hondt, S.L., and Miller, D.J. (Eds.), *Proc. ODP, Sci. Results*, 201, 1–21 [Online]. Available from World Wide Web: <[http://www-odp.tamu.edu/publications/201\\_SR/VOLUME/CHAPTERS/114.PDF](http://www-odp.tamu.edu/publications/201_SR/VOLUME/CHAPTERS/114.PDF)>. [Cited YYYY-MM-DD]

<sup>2</sup>Monterey Bay Aquarium Research Institute, 7700 Sandholdt Road, Moss Landing CA 95039-9964, USA.

Correspondence author:

[methane@mbari.org](mailto:methane@mbari.org)

<sup>3</sup>Integrated Ocean Drilling Program, 1000 Discovery Drive, College Station TX 77845-9547, USA.

Initial receipt: 26 July 2004

Acceptance: 7 June 2005

Web publication: 18 January 2006

Ms 201SR-114

development of the tool, its design, and initial tests of the tool conducted at ODP Site 1226.

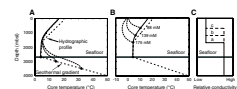
During the more than a quarter century of Deep Sea Drilling Project (DSDP) and ODP drilling, vigorous gas expansion and anomalously cold temperatures in cores from continental margins have been commonly observed. Thermal observations have included cores feeling cold (e.g., Leg 146, Site 889 [Westbrook, Carson, Musgrave, et al., 1994]) and the presence of frozen pore waters along the interior wall of the core liner (e.g., Leg 164 [Paull, Matsumoto, Wallace, et al., 1996]). A few investigations have quantified these observed thermal anomalies by inserting thermistors into the core after it has been removed from the core barrel and delivered to the catwalk (Leg 164, Site 994 [Paull, Matsumoto, Wallace, et al., 1996]) or to the core laboratory immediately after core splitting (temperatures as low as  $-2^{\circ}\text{C}$  have been recorded) (e.g., Leg 66, Site 490 [Watkins, Moore, et al., 1982]; Leg 146, Site 889 [Westbrook, Carson, Musgrave, et al., 1994]) and by scanning core liner on the catwalk with infrared imaging cameras (e.g., Leg 201 [Ford et al., 2003]; Leg 204 [Trehu et al., 2004]). These “catwalk core temperature” measurements show that some core sections arrived on deck at distinctly lower temperatures ( $5^{\circ}$ – $10^{\circ}\text{C}$  cooler) than other cores recovered from the same drill site.

As part of the shipboard sampling protocol used during DSDP and ODP, core gas samples have been collected soon after the core arrived on deck for routine gas chromatographic analysis of the low molecular weight gases, including methane. Gas composition data clearly indicate that core gas is usually dominated by methane. However, because most of the dissolved and interstitial gas contained in sediment cores is lost during their ascent to the surface (e.g., Paull and Ussler, 2000), very little is known about how much methane was actually in these sediments before recovery. This gas loss and the thermal anomalies observed soon after core recovery suggest that the temperature history of a gas-rich sediment core may provide information about the amount of gas originally contained in the sediment prior to recovery.

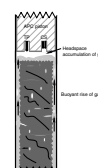
There are three endothermic processes that can cause a temperature decrease in sediment cores during their ascent to the sea surface: (1) gas expansion, (2) gas exsolution, and (3) gas hydrate decomposition. Predictions about the temperature changes that will occur in gassy sediments (with or without gas hydrates) during core recovery based on simple thermodynamic calculations (Ussler et al., 2002) indicate that temperature changes caused by a combination of one or more of these endothermic processes are of the right order of magnitude and direction (i.e.,  $1^{\circ}$ – $10^{\circ}\text{C}$  colder than gas-free sediment).

Thermal modeling has shown that cores which evolve gas during their ascent to the surface will have distinct ascent temperature profiles (Fig. F1) (Ussler et al., 2002). Ascent temperature profiles will track profiles for gas-free cores until gas saturation occurs and exsolution commences. Free gas coming out of solution along the length of the core will buoyantly rise within the core barrel (Fig. F2). As soon as free gas is trapped at the top of the core barrel, temperatures should drop as a result of gas exsolution and gas expansion (Fig. F1B). Most of the gas exsolution and expansion, and thus the largest temperature changes, will occur in the upper water column. In situ gas concentration can be calculated using the pressure and temperature of the inflection in ascent temperature profiles and the methane gas solubility model of Duan et al. (1992), assuming that no gas was introduced during the coring process.

F1. Radial heat transfer models of ascent temperatures, p. 11.



F2. Upper portion of an APC core barrel, p. 12.



The in situ gas concentrations at Site 1226 are believed to be considerably less than those needed to achieve gas saturation of the pore water during core recovery because (1) no observations of core degassing or anomalously low core temperatures were made at this site, (2) the cores contain sulfate throughout (22–30 mM), and (3) the measured methane gas concentrations were low (<2  $\mu\text{M}$ ) (D'Hondt, Jørgensen, Miller, et al., 2003). No gas exsolution from the sediments should occur during core ascent to the surface at this site. Therefore, Site 1226 is viewed as a gas-poor background site suitable for determining the response of the TPC tool without the additional complexity of thermal and pressure effects associated with the presence of gas.

In the Leg 201 *Initial Reports* volume (D'Hondt, Jørgensen, Miller, et al., 2003), the TPC tool was renamed the APC-Methane (APC-M) tool. Although this fits better with the naming convention used by ODP, this is an unfortunate misnomer because the tool neither detects methane nor measures its concentration. Because the original National Science Foundation (NSF) proposal and previous publications (Ussler et al., 2000, 2001, 2002, 2003) described the tool as the TPC, we will continue using this name because of its more accurate description of what is measured.

## METHODS

### Temperature, Pressure, and Conductivity Tool

The TPC tool is designed to continuously record temperature, pressure, and conductivity at the face of a modified ODP APC piston assembly (Figs. F2, F3, F4) during deployment, core collection, and recovery. The APC piston was modified to contain the TPC tool components (Fig. F3), and the tool has a maximum design pressure of 10,000 psi, which corresponds to ~6.9 km total hydrostatic depth.

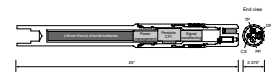
Making measurements at the piston face allows for standardization of the effects of cooling during core ascent. This location was chosen for practical reasons: (1) the APC piston could be easily modified to incorporate TPC sensors; (2) the data logging electronics and battery could be housed in the existing piston corer subassembly, making this an autonomous downhole tool; (3) no special downhole tool runs would be necessary to collect TPC data, causing little disruption to the tempo of coring operations; and (4) gas can collect in a recess on the piston face, making electrical conductivity measurements possible.

Because there is a large contrast in electrical properties between a gas phase (lower conductivity) and wet sediment and/or seawater (higher conductivity), the conductivity sensor was designed to detect the formation of a headspace gas phase at the top of a sediment core (Fig. F2). This information aids in analyzing the temperature and internal pressure data obtained during core ascent by providing an independent confirmation of headspace formation.

### Sensors

The temperature and conductivity sensors are recessed in shallow wells on the piston face for mechanical protection and for the accumulation of a headspace gas phase (Figs. F2, F3, F4). The pressure port opens directly onto the face of the APC piston. The sensors are threaded into the sensor head for ease of replacement.

F3. APC piston containing the TPC tool, p. 13.



F4. End view of the APC piston, p. 14.



Temperature is measured using a YSI 55036 thermistor encapsulated within a thin-walled stainless steel probe ( $3/16$  in diameter  $\times$   $1/4$  in long) with a pressure rating of 10,000 psi (Logan Enterprises, West Liberty, Ohio, USA). The time constant for this thermistor probe is 1.5 s, and the accuracy is  $\pm 0.05^\circ\text{C}$ . Pressure is measured using a transducer designed for use in corrosive downhole environments and for temperature stability (model 211-37-520; Paine Corp., Seattle, Washington, USA). Measurement error is  $\pm 0.15\%$  of the full-scale reading of 10,000 psi. The conductivity probe is a miniature bulkhead connector with an inconel body and three gold-plated 0.040-in-diameter Kovar pins (PMS-series; Kemlon Products and Development, Pearland, Texas, USA). Pin spacing is 3.2 mm.

## **Electronics**

Design objectives for the electronics included minimal power consumption, low component count, 12-bit or better analog-to-digital (A/D) resolution, low long-term sensor drift, vibration tolerance, large amounts of nonvolatile data storage, and ease of programming and component replacement. Three elements compose the electronics package: (1) the sensor conditioning electronics, (2) an off-the-shelf microprocessor unit, and (3) the batteries. Low-power 3.3-V CMOS semiconductor components were selected to minimize current drain. The discrete components are surface-mounted on a narrow multilayer printed circuit board that supports the detachable microprocessor unit. To prevent polarization of the conductivity electrodes, the conductivity sensor is excited using an alternating-current signal generated by a simple oscillator circuit. After signal conditioning, the analog signals from the sensors are fed into either a Maxim MAX147 12-bit A/D converter (thermistor and conductivity) or a Cirrus CS5509 16-bit A/D converter (pressure). These A/D converters are connected to a Persistor CF1 microprocessor unit via the Queued Serial Peripheral Interface implemented by the Motorola 68338 central processing unit. Data are stored in a 48-MB CompactFlash card hardwired to the CF1 microprocessor unit. Communications with the CF1 occurs through an RS-232 interface. The CF1 is programmed in C, using the Metrowerks CodeWarrior programming environment. TPC data were collected at 1-s intervals throughout tool deployment.

Power is supplied by two double-C lithium thionyl chloride batteries within a 1-in-diameter  $\times$  9-in-long battery pack that provides 7.3 V with a 100-mA rating. The electronics/battery assembly was designed for no less than 100 hr of continuous operation.

Data transfer can be accomplished while the TPC tool is installed in the APC drilling string through a RS-232 communications port on the face of the piston. This data port is a three-pin keyed bulkhead connector (PMJ-series; Kemlon Products and Development, Pearland, Texas, USA). During coring operations, this port is O-ring sealed with a faceplate that is easily removed for access (Fig. F4).

## **DATA REDUCTION**

Raw TPC temperature data were converted to thermistor resistance ( $R$ , ohms) using a fourth-order polynomial equation fit with empirically derived calibration coefficients:

$$R = (5.95445 \times 10^{-10} \text{ counts})^4 + (-8.03615 \times 10^{-6} \text{ counts})^3 + (4.23147 \times 10^{-2} \text{ counts})^2 + (-1.08555 \times 10^2 \text{ counts}) + (1.25574 \times 10^5). \quad (1)$$

Temperature ( $K$ ) was calculated from thermistor resistance using the Steinhart and Hart relationship (Anonymous, 1980):

$$1/T = A + B(\ln R) + C(\ln R)^3. \quad (2)$$

The manufacturer-supplied coefficients for the thermistor used for all the tool runs at Site 1226 (serial number 0047-25) are

$$\begin{aligned} A &= 1.133852001 \times 10^{-3}, \\ B &= 2.334260615 \times 10^{-4}, \text{ and} \\ C &= 9.056721961 \times 10^{-8}. \end{aligned}$$

TPC pressure in psig was computed from raw bit count data using an empirically derived constant = 0.1785 psi/bit. Because local hydrographic profiles were not obtained, depth (meters below sea level [mbsl]) was computed from measured pressure (psig), assuming an average seawater density of 1.025 g/cm<sup>3</sup>.

Output from the conductivity sensor was digitized by the 12-bit Maxim MAX147 A/D converter, and values were recorded as raw bit counts. Because the conductivity circuit was designed to avoid polarization and electrode corrosion in seawater, measured values oscillate rapidly between two extreme values. A change in the difference between the minimum and maximum values indicates a change in the conductivity of the medium contacting the electrodes. Conductivity data for each sensor were normalized by subtracting the mean value from each data point and then taking the absolute value. These normalized conductivity values, expressed in bits, should not be confused with standard seawater conductivity measurements. Large values of normalized conductivity correspond to a gas headspace and small values correspond to the presence of seawater at the sensor electrodes. This is the opposite of what would be expected and is simply an artifact of the sensor electronics. Visual calibration of the conductivity signal was accomplished during a Monterey Bay Aquarium Research Institute remotely operated vehicle dive in October 2000 using an actual TPC tool assembly.

## RESULTS

The TPC tool was deployed in Hole 1226B continuously from Cores 201-1226B-5H through 20H but stopped recording data after Core 10H. No reason for this interruption in recording was determined. In Hole 1226E, TPC data were recorded continuously from Cores 201-1226E-5H through 12H. Raw and derived TPC data are compiled in Tables T1 (Hole 1226B) and T2 (Hole 1226E). Seafloor depth for Hole 1226B was 3297.0 mbsl, and depth for Hole 1226E was 3296.4 mbsl.

---

T1. Raw and derived data, Hole 1226B, p. 19.

---



---

T2. Raw and derived data, Hole 1226E, p. 20.

---

## Site 1226: Descent and Ascent Temperature Profiles

Temperature-pressure-depth profiles for each tool run are illustrated in Figure F5A (Hole 1226B) and F5B (Hole 1226E). Descent profiles from both holes show steady decreases in temperature from ~28°C surface waters to bottom temperatures between 2° and 11°C. These data show that the TPC tool has a significant temperature (thermal) lag during descent.

Ascent temperature profiles are more complicated. Ascent temperature profiles begin at temperatures between 5° and 10°C, and temperature decreases during ascent toward warmer surface waters. These decreases in temperature become more rapid during the midportion of the ascent profile for most cores, and with the exception of Cores 201-1226E-7H, 9H, and 11H, temperatures in the headspace of the core become colder than those in the water column, as indicated by the regional hydrographic profile.

For most of the descent and ascent profiles, rates of wireline movement are steady (Fig. F6). Thus, the thermal signals during core descent and ascent are the result of the temperature structure of the ocean water and thermal changes in the headspace inside the APC and not the consequence of erratic core movement in the water column.

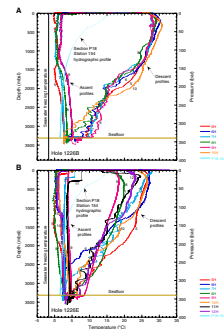
## In-Hole Pressure and Temperature Signals

Distinct pressure and temperature variations occur when an APC core is collected (Fig. F7). During core descent, temperature decreased rapidly and somewhat erratically as the cooler deep ocean water was entered. The APC was generally held suspended at the seafloor for a few minutes before being lowered to the mudline or in the borehole at the mudline. While the APC wireline was stabilizing in the borehole, temperature slowly decreased toward bottom water temperature (~1.7°C). Once the APC attained a stable depth in the borehole, a core was taken by pumping against the coring string with the mud pumps and a shear pin broke at a predetermined pressure differential. The pressure data show that when this shear pin breaks, a pressure oscillation is generated with a range of ~8 bar that often lasts for >3 min with no apparent temperature change. At the time of APC pullout, another comparable 6- to 8-bar pressure oscillation of similar duration was generated and a negative temperature anomaly was produced (Fig. F7). When viewed in detail, this temperature anomaly, which varies in size from a few tenths of a degree to 2°C in any individual core, is correlated with the pressure reduction spike created at the time of core pullout. Once core ascent begins, pressure inside the headspace appears to track the ambient pressure outside the APC. Although we do not have independent wireline length data to determine where the TPC tool was located in the drill pipe, pressure oscillations and deviations from ambient pressure appear to be small at Site 1226.

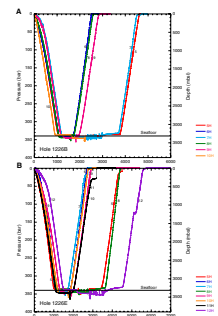
## Conductivity Measurement

Conductivity measurements show when gas headspace forms at the face of the TPC tool. High normalized conductivity measurements, indicating the presence of headspace gas, were noted during many runs. Figure F8 illustrates an example of a tool run (Core 201-1226E-12H) that detected the disappearance and reappearance of a gas headspace. Table T3 summarizes the depths at which similar disappearances and

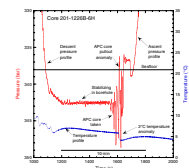
F5. Pressure-depth-temperature profiles, p. 15.



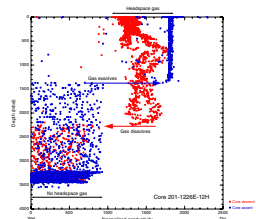
F6. Pressure and depth vs. time profiles, p. 16.



F7. Temperature and pressure changes during core collection, p. 17.



F8. Conductivity data, p. 18.



T3. Headspace gas fluctuations, p. 21.



reappearances of gas headspace occurred during all the TPC tool runs. Cores with the shallowest depths of gas headspace disappearance (<300 mbsl) were essentially devoid of gas. In all cases, the conductivity data show that gas was initially carried down into the borehole with the tool, and in many cases, the tool never lost this gas headspace during the entire run (e.g., Cores 201-1226B-5H, 7H, and 10H and 201-1226E-8H and 10H). During other tool runs, the pattern of gas headspace occurrence is more complicated. In almost all cases when gas headspace disappears and reappears during core ascent, the depth at which the headspace reappears is less than the depth at which it disappeared during core descent (Table T3), indicating that there has been a net loss of gas from the seawater immediately in front of the face of the TPC tool.

Cores 201-1226B-5H and 7H and 201-1226E-5H and 8H had the coolest temperatures of all cores from Site 1226 (between 700 and 1800 mbsl). Conductivity data indicate that gas headspace was present throughout the coring. However, Core 201-1226E-5H did lose and regain headspace. In two cases, a temperature decrease was associated closely in depth with headspace formation (Cores 201-1226E-5H at ~1950 mbsl and 12H at ~1150 mbsl) (Fig. F5B; Table T3). The temperature excursion in Core 201-1226E-6H during ascent occurred at ~1100 mbsl after conductivity data indicated gas headspace was reestablished.

## DISCUSSION

Headspace temperature curves obtained using the TPC tool are the first systematic attempt to record the temperature inside a coring system during core recovery. Some ascent curves show thermal phenomena that would be anticipated for gas-bearing cores. Understanding the source of this gas is critical for interpreting the TPC data. A geological source for the observed gas is excluded because sediment gas data for Site 1226 show no indication of significant quantities of methane gas in these sediments. Methane concentrations in the uppermost 100 mbsf at Site 1226 are <2  $\mu\text{M}$  and sulfate concentrations span from 22 to 30 mM (D'Hondt, Jørgensen, Miller, et al., 2003). These concentrations are consistent with low to modest levels of microbial activity and do not suggest that any substantial accumulations of methane should be expected in this sedimentary section. Thus, the gas detected by the TPC tool was introduced at the surface.

Conductivity measurements indicate that, in every case, gas is trapped in headspace at the face of the TPC tool during the *initial* deployment of the tool downhole. In many cases, the conductivity sensor indicates that the gas headspace disappeared during descent and reappeared during ascent, albeit at a slightly shallower depth. This suggests that gas completely dissolved during descent and then exsolved during ascent. There are no cases where the initial headspace did not return during ascent, whereas in some cases the gas headspace never completely disappeared. However, the conductivity data for three cores that have the earliest disappearance and latest reappearance of a gas headspace (Cores 201-1226E-7H, 9H, and 11H) indicate very little gas was entrained under the face of the TPC tool during these particular runs. The ascent temperature profiles for these curves (Fig. F5B) lack any signal related to gas exsolution or expansion. Thus, the size of the initial trapped gas headspace is quite variable, but it is always present during APC coring.

The trapping of gas headspace at the face of the TPC tool when the tool is first deployed is most likely the natural consequence of the coring process. While the drill pipe is opened for insertion of the APC coring string, the level of seawater in the pipe drains down from the rig floor to sea level, a distance of 11.2 m. When the drill pipe is reassembled, ~100 L of atmospheric gas is trapped within the drill pipe. This trapped gas is circulated down the hole by the mud pumps and eventually should exit at the seafloor. However, the conductivity data suggest sufficient amounts of gas remain trapped and/or dissolved in the seawater adjacent to the TPC tool to affect the conductivity sensor. Undoubtedly, this gas contributes to the thermal signal measured by the TPC thermistor (Fig. F5). This entrainment of atmospheric gases into the coring system is also the most likely explanation for some runs of the Pressure Core Sampler (PCS) during Leg 201 coming up with pressurized air (J. Dickens, pers. comm., 2003; Dickens et al. 2003). Changes in coring protocols will be necessary to alleviate this inherent flaw in pressure coring techniques.

The TPC data obtained from Site 1226 establish a baseline for the types of effects that would be expected during APC coring of known gas-rich sites. At gas-rich sites, the addition of gas from sedimentary sources should create a different pattern of conductivity changes. A conductivity change during core ascent at depths greater than those for core descent would be a clear indication of gas addition. Because gas was initially entrained in the coring system during its descent in the drill pipe, the temperature anomalies measured at Site 1226 during core ascent define the limits on the range of thermal changes that can be expected for cores collected at gas-rich sites. Data from Site 1226 have shown that there are wide variations in what happens with gas in cores, and more data are required to determine why these variations occur. Cores that remained at the bottom of the borehole the longest before being pulled out had the greatest depth difference between the disappearance and reappearance of a gas headspace. Mud pump circulation, which is always maintained while a coring string is in a borehole, may have swept out some of the gas entrained by the APC coring system.

Relatively small (<8 bar) pressure anomalies were produced within the core liner of cores collected at Site 1226. In numerous cases, there was a pressure increase when the APC was shot into the sediment and a pressure decrease when the core was pulled out. The core pullout caused gas expansion within the core liner, rapidly creating a relatively large (up to 2°C) temperature anomaly that decayed quickly as the core ascended to the surface.

A benefit derived from the temperature and pressure data collected by the TPC tool is improved understanding of the core recovery process. Collecting the APC core creates temperature and pressure anomalies that have the potential to alter the physical state of the core material and may lead to expanded core recovery statistics (>100%). When more data become available from sites with different lithologies, we may learn more about how the coring process could be modified to enhance core recovery and quality.

## **SUMMARY AND CONCLUSIONS**

TPC data collected at Site 1226 demonstrate how the tool performs at a gas-poor background site in a relatively deepwater setting. The ascent profiles document thermal changes consistent with the occurrence of



gas at the face of the TPC tool. Conductivity data and observations of drilling technique show that headspace gas is trapped at the face of the TPC tool during every deployment of the APC coring string; thus, the observed thermal changes during core ascent are the natural consequence of normal coring operations. Because the depth at which the gas headspace reappeared was less than the depth where it disappeared, it is believed that the entrained gas was partially flushed away during operation of the mud pumps. This inadvertent pumping of atmospheric gases down the drill pipe complicates the use of this tool and other gas-collecting tools (e.g., the PCS and the hydrate autoclave coring equipment). These tools have been developed and operated anticipating that the introduction of atmospheric gases into the bottom of a borehole does not occur.

Pressure anomalies formed during core withdrawal may provide insight into APC core expansion. Excess recovery (>100% length) of APC cores is common and may be the result of the negative pressure anomalies generated during core pullout.

The TPC tool recorded thermal and conductivity signatures of gas evolution, and temperature ascent profiles that are consistent with models of what gas evolution would look like in gas-rich sediments cores.

## **ACKNOWLEDGMENTS**

This research used samples and/or data provided by the Ocean Drilling Program (ODP). ODP is sponsored by the U.S. National Science Foundation (NSF) and participating countries under management of Joint Oceanographic Institutions (JOI), Inc. Funding for this research was provided by the NSF (OCE-9910418) and the David and Lucile Packard Foundation. We thank Thomas Sullivan, Persistor Corporation, for assistance with implementation of the QSPI interface on the CF1. Jerry Dickens and Alexi Milkov provided helpful reviews.

## REFERENCES

- Anonymous, 1980. *Practical Temperature Measurements, Application Note 290*: Santa Clara, CA (Hewlett-Packard Corp.). Available from World Wide Web: <<http://cp.literature.agilent.com/litweb/pdf/5965-7822E.pdf>>. [Cited 2000-09-02]
- D'Hondt, S.L., Jørgensen, B.B., Miller, D.J., et al., 2003. *Proc. ODP, Init. Repts.*, 201 [CD-ROM]. Available from: Ocean Drilling Program, Texas A&M University, College Station TX 77845-9547, USA. [HTML]
- Dickens, G.R., Schroeder, D., Hinrichs, K.-U., and the Leg 201 Scientific Party, 2003. The pressure core sampler (PCS) on ODP Leg 201: general operations and gas release. In D'Hondt, S.L., Jørgensen, B.B., Miller, D.J., et al., *Proc. ODP, Init. Repts.*, 201, 1–22 [Online]. Available from World Wide Web: <[http://www-odp.tamu.edu/publications/201\\_IR/VOLUME/CHAPTERS/IR201\\_03.PDF](http://www-odp.tamu.edu/publications/201_IR/VOLUME/CHAPTERS/IR201_03.PDF)>. [Cited 2005-05-03]
- Duan, Z., Møller, N., Greenberg, J., and Weare, J.H., 1992. The prediction of methane solubility in natural waters to high ionic strengths from 0° to 250°C and from 0 to 1600 bar. *Geochim. Cosmochim. Acta*, 56:1451–1460.
- Ford, K.H., Naehr, T.H., Skilbeck, C.G., and the Leg 201 Scientific Party, 2003. The use of infrared thermal imaging to identify gas hydrate in sediment cores. In D'Hondt, S.L., Jørgensen, B.B., Miller, D.J., et al., *Proc. ODP, Init. Repts.*, 201 [Online]. Available from World Wide Web: <[http://www-odp.tamu.edu/publications/201\\_IR/chap\\_04/chap\\_04.htm](http://www-odp.tamu.edu/publications/201_IR/chap_04/chap_04.htm)>. [Cited 2005-05-03]
- Paull, C.K., Matsumoto, R., Wallace, P.J., and Dillon, W.P. (Eds.), 1996. *Proc. ODP, Sci. Results*, 164: College Station, TX (Ocean Drilling Program). [HTML]
- Paull, C.K., and Ussler, W., III, 2000. History and significance of gas sampling during DSDP and ODP drilling associated with gas hydrates. In Paull, C.K., and Dillon, W.P. (Eds.), *Natural Gas Hydrates: Occurrence, Distribution, and Detection*. Am. Geophys. Union, Geophys. Monogr. Ser., 124:53–66.
- Trehu, A.M., Long, P.E., Torres, M.E., Bohrmann, G., Rack, F.R., Collett, T.S., Goldberg, D.S., Milkov, A.V., Riedel, M., Schultheiss, P., Bangs, N.L., Barr, S.R., Borowski, W.S., Claypool, G.E., Delwiche, M.E., Dickens, G.R., Gracia, E., Guerin, G., Holland, M., Johnson, J.E., Lee, Y.-J., Liu, C.-S., Su, X., Teichert, B., Tomaru, H., Vanneste, M., Watanabe, M., and Weinberger, J.L., 2004. Three-dimensional distribution of gas hydrate beneath southern Hydrate Ridge: constraints from ODP Leg 204. *Earth Planet. Sci. Lett.*, 222:845–862.
- Ussler, W., III., Paull, C.K., McGill, P., Schroeder, D., and Ferrell, D., 2001. Estimating in situ sediment gas concentrations in ODP boreholes by continuously monitoring temperatures during core recovery. *Eos, Trans. Am. Geophys. Union*, 82:S445–S446.
- Ussler, W., III., Paull, C.K., McGill, P., Schroeder, D., and Ferrell, D., 2002. Estimating in situ sediment gas concentrations in ODP boreholes by continuously monitoring temperature during core recovery. *Proc. 4th Int. Conf. Gas Hydrate*, 1:210–215.
- Ussler, W., III., Paull, C.K., McGill, P., Schroeder, D., Ferrell, D., and Leg 201 and 204 Scientific Parties, 2003. Estimates of in situ sediment gas concentrations in ODP boreholes from records of core temperature obtained during core recovery. *Geophys. Res. Bull.*, 5:02964. (Abstract)
- Ussler, W., III., Paull, C.K., McGill, P., Schroeder, D., and Friederichs, M., 2000. A new approach for estimating in situ sediment gas concentrations in ODP boreholes while coring. *GSA Bull.*, 32:A102. (Abstract)
- Watkins, J.S., Moore, J.C., et al., 1982. *Init. Repts. DSDP*, 66: Washington (U.S. Govt. Printing Office).
- Westbrook, G.K., Carson, B., Musgrave, R.J., et al., 1994. *Proc. ODP, Init. Repts.*, 146 (Pt. 1): College Station, TX (Ocean Drilling Program).

**Figure F1. A, B.** Results of radial heat transfer models of ascent temperature paths that would be followed during core recovery. The most important control on heat transfer is the plastic core liner, which has very low relative thermal conductivity ( $11.3 \text{ J/min}\cdot\text{m}\cdot^\circ\text{C}$ ). The broadly spaced dashed line in A and B is a combined hydrographic geothermal temperature profile. In A, three profiles from non-gassy cores are shown, which differ by their initial temperature. The mud-line core (2700 mbsl) is represented by the solid line, and both the 3000 and 3500 mbsl cores are shown with tightly spaced dashed lines. Thus, all gas-free cores from a drill site should have the same thermal overprinting and their recovery temperatures are indistinguishable. B shows thermal signatures generated by cores with varying amounts of initial interstitial methane gas concentrations. These curves converge with and follow the mudline core temperature path (solid line) until gas bubbles are generated. When gas bubble formation occurs, the temperature profiles show a distinct cooling. C. Corresponding records of relative conductivity (unitless) predicted for the thermal paths indicated in B ( $a = 175 \text{ mM}$ ,  $b = 139 \text{ mM}$ ,  $c = 88 \text{ mM}$ ), shown schematically. Low conductivity indicates the presence of gas headspace; high conductivity indicates the conductivity electrodes are bathed in seawater or mud. A sudden decrease in relative conductivity is expected to occur as soon as headspace gas volume has been generated.

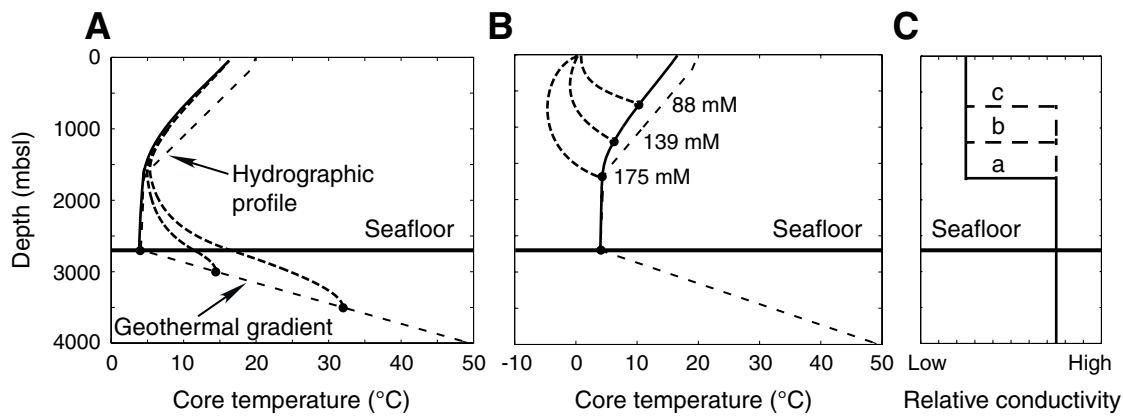
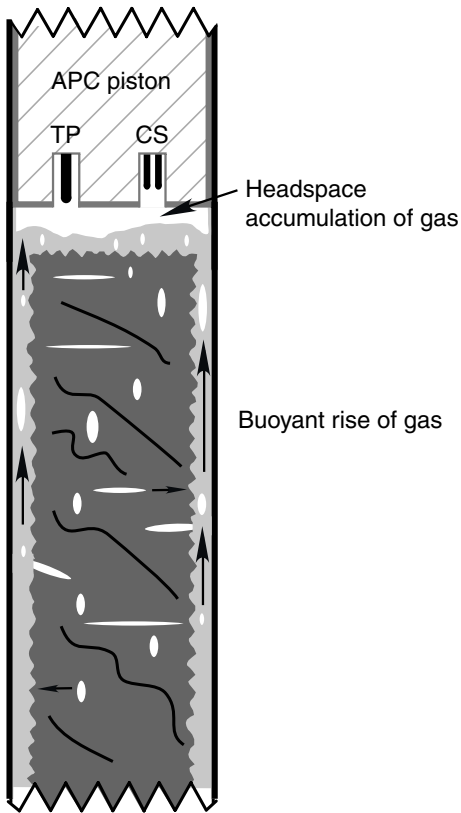


Figure F2. Schematic cross section of the upper portion of an advanced piston corer (APC) core barrel filled with a sediment core, illustrating how gas bubbles will migrate out of the sediment and move upward along the side of the core liner to accumulate at the top of the core barrel under the face of the APC piston. TP = thermistor probe, CS = conductivity sensor.



**Figure F3.** Schematic cross section and end view of the APC piston containing the TPC tool. The end view of the APC piston face shows the arrangement of the TPC sensors. TP = thermistor probe, CS = conductivity sensor, PP = pressure port, DP = data dump port. The data dump port is sealed during deployment but is available for data downloads on the drillship catwalk.

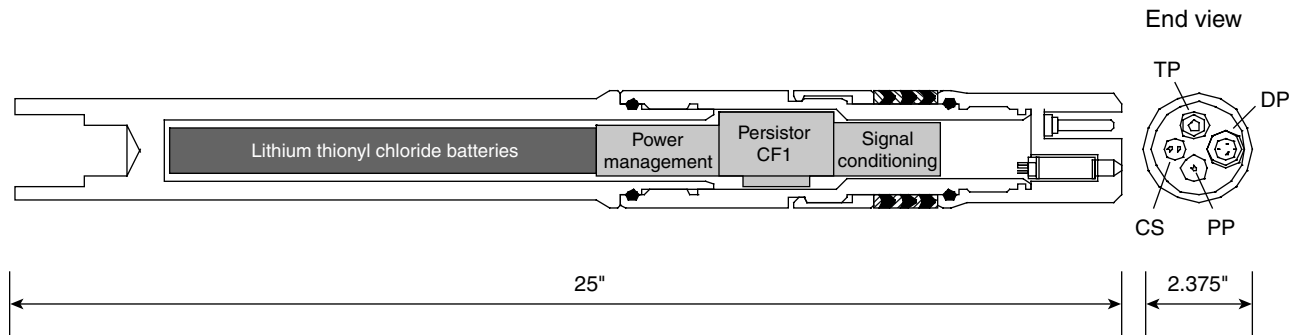


Figure F4. End view of the APC piston (Fig. F3, p. 13), showing placement of sensors and ports.

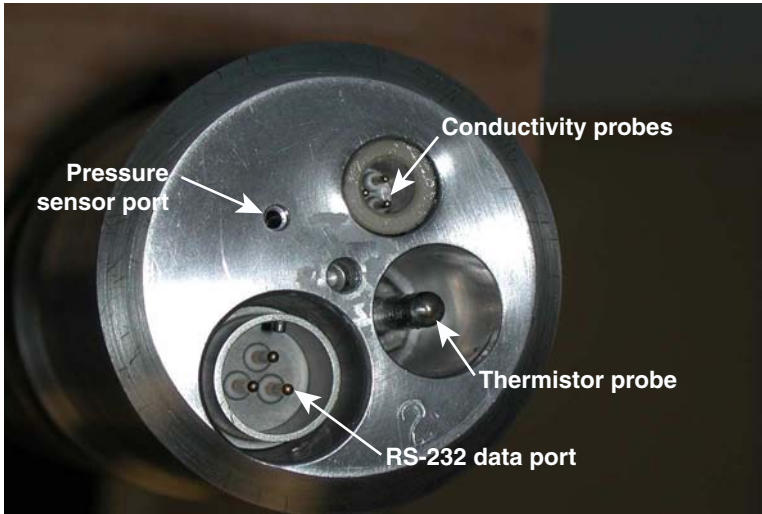
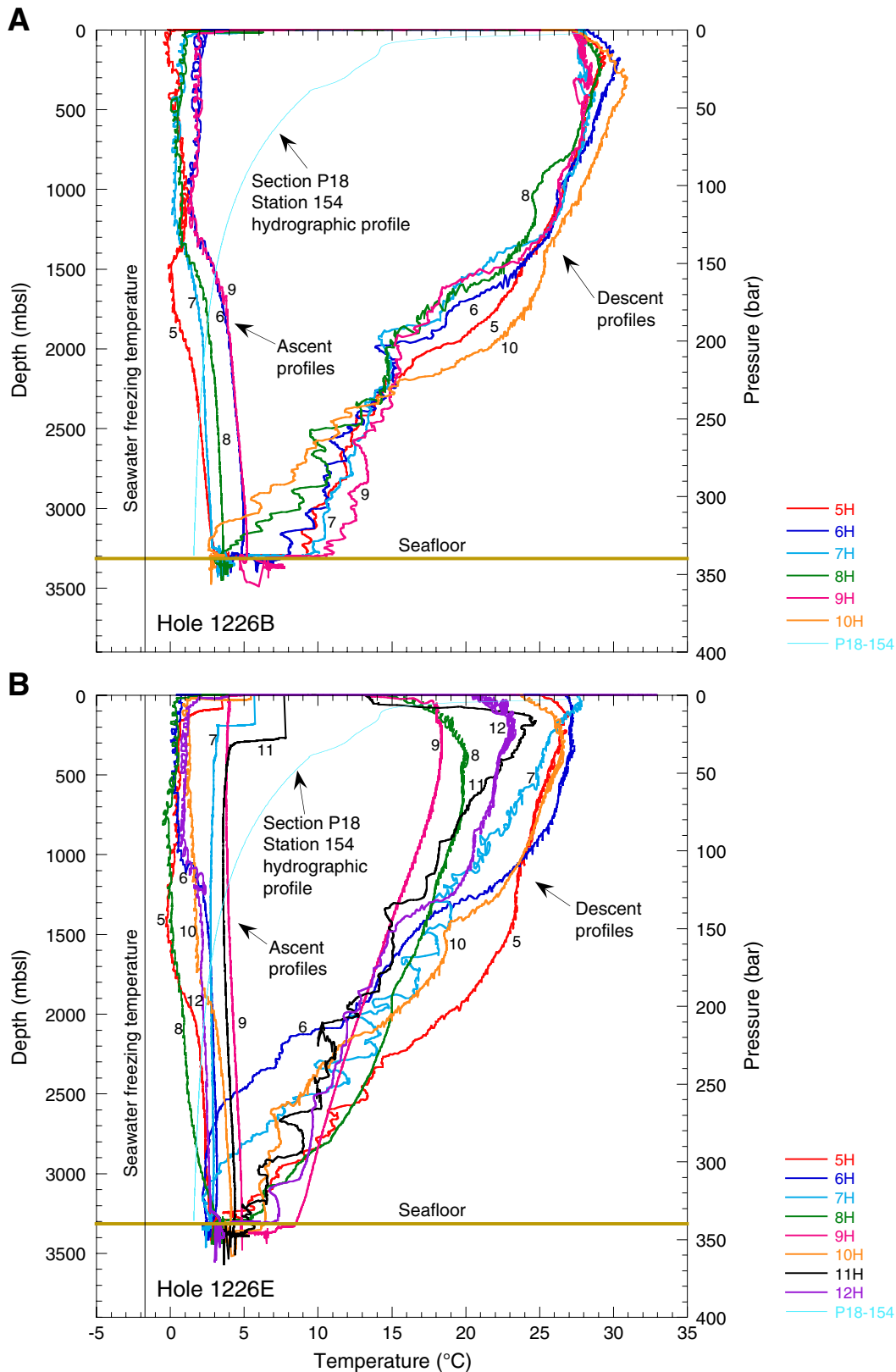




Figure F5. Pressure-depth-temperature profiles for Holes (A) 1226B and (B) 1226E. A hydrographic profile from WOCE Section P18N Station 154 ([whpo.ucsd.edu/data/onetime/pacific/p18/p18su.txt](http://whpo.ucsd.edu/data/onetime/pacific/p18/p18su.txt)) in 3770 m of water, located at 3°N, 110°20' W is shown for comparison. Pressure was measured and depth was calculated as described in the text.



**Figure F6.** Pressure and depth vs. time profiles for Holes (A) 1226B and (B) 1226E. Mean ( $\pm 1\sigma$ ) rates were calculated along the linear portion of the profiles between 1500 and 3000 m. Mean descent rate for Hole 1226B =  $235 \pm 5$  m/min; the ascent rate =  $240 \pm 5$  m/min. Mean descent rate for Hole 1226E =  $227 \pm 15$  m/min; the ascent rate =  $219 \pm 13$  m/min. Pressure was measured and depth was calculated as described in the text.

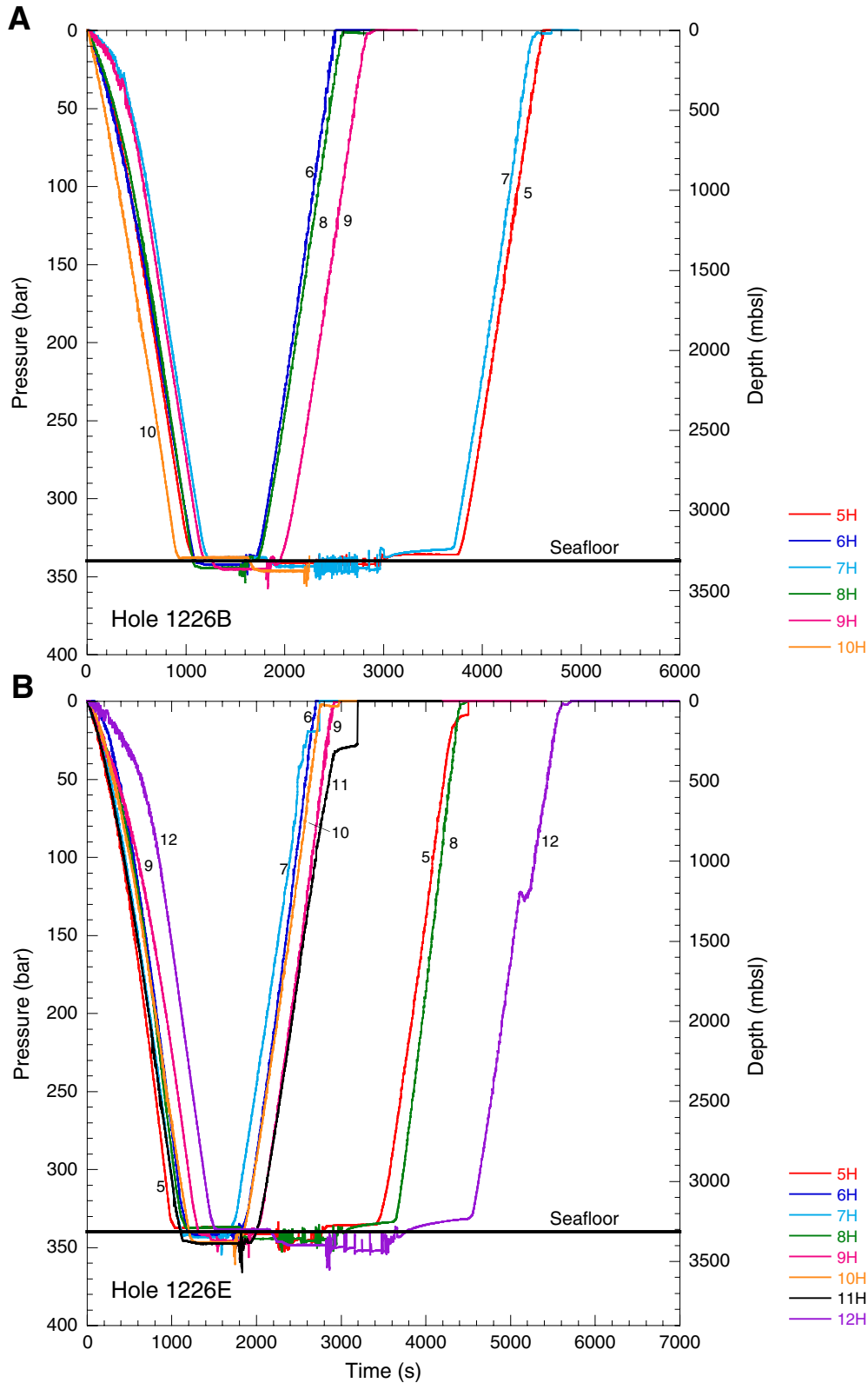
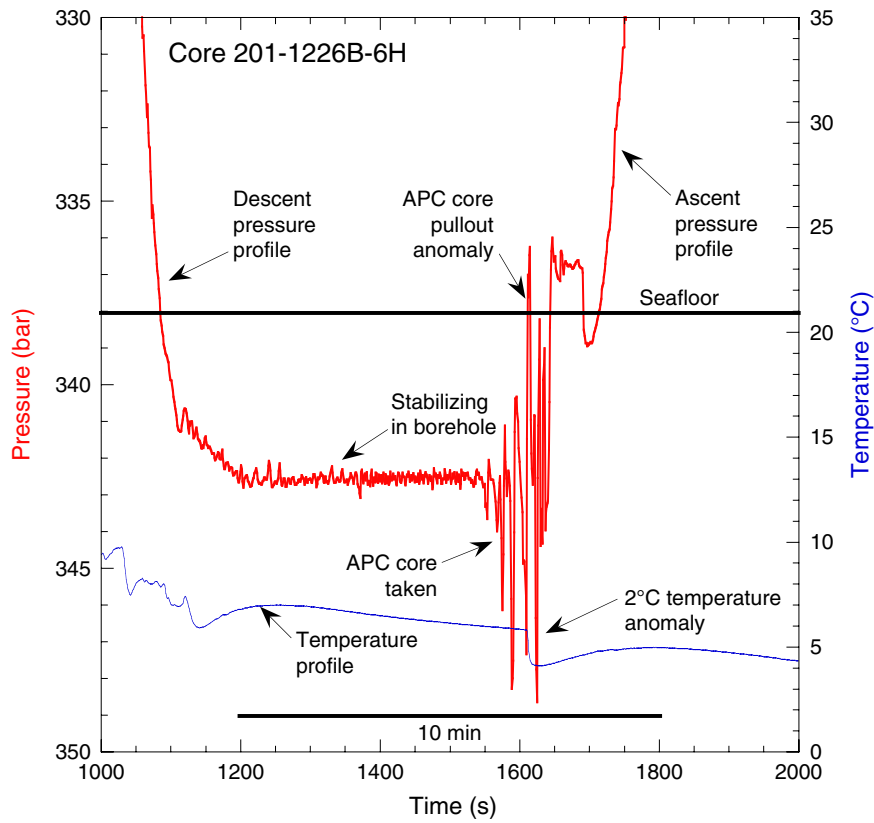


Figure F7. Example of the temperature and pressure changes that occur during core collection, illustrated using data from Core 201-1226B-6H. Pressure oscillations are related to recovery of internal core pressure conditions after shooting the advanced piston corer (APC) into the sediment and its subsequent withdrawal.



**Figure F8.** Example of conductivity data collected for Core 201-1226E-12H. High values of conductivity (>1100 bits) correspond to the occurrence of headspace gas at the top of the APC core (dry) and lower values (<1000 bits) indicate the loss of headspace gas and contact of the conductivity electrodes with seawater (wet). This sensor response is opposite from that expected for seawater conductivity measurements and is simply an artifact of the sensor electronics. The data show that the core begins its descent into the drill pipe with headspace gas. An abrupt change in conductivity occurs at 2250 mbsl, indicating the complete disappearance of headspace gas in contact with the face of the TPC tool. During the return of the core to the surface, headspace gas reforms abruptly at 1360 mbsl and is maintained to the rig floor.

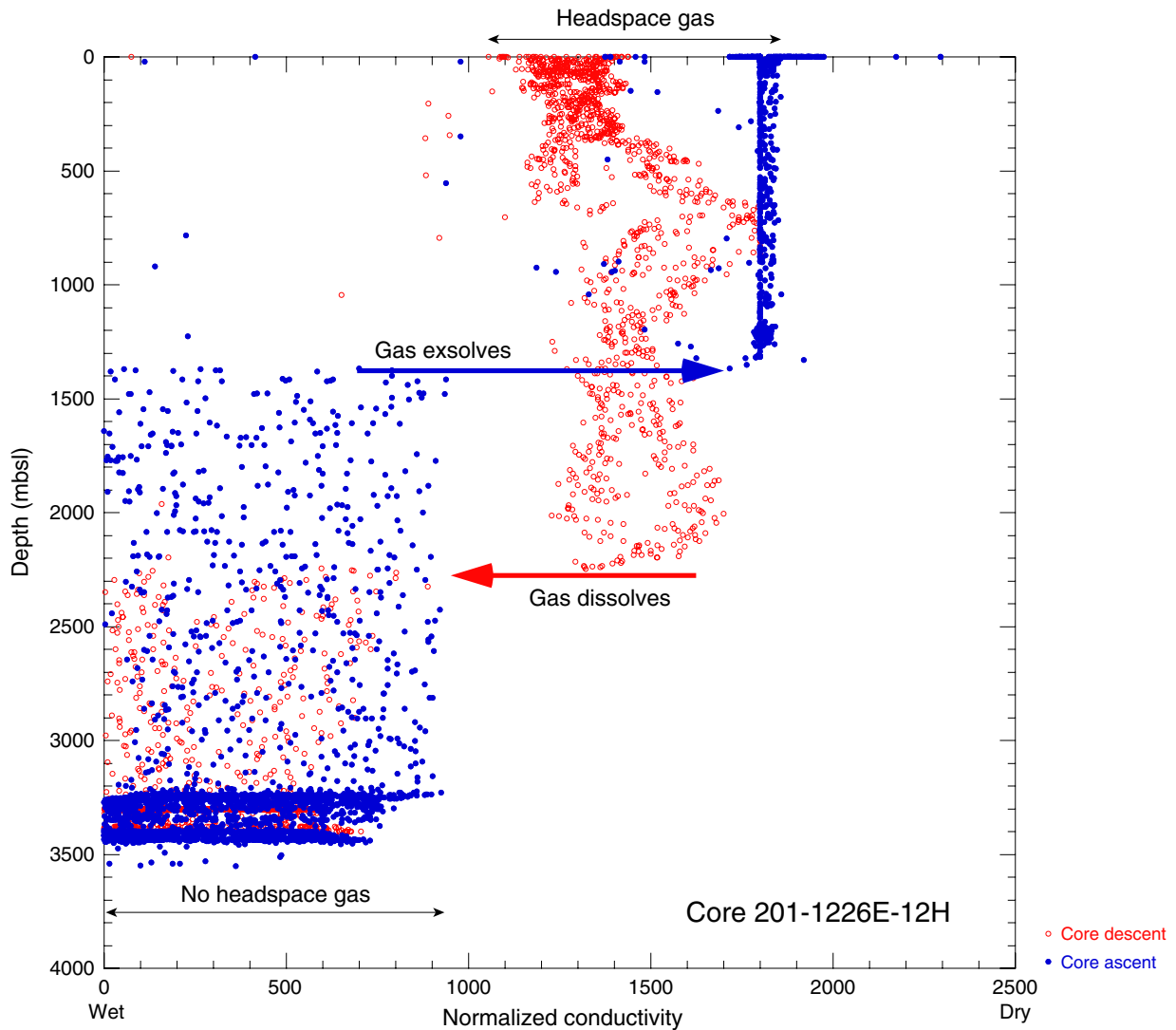


Table T1. Raw and derived data, Hole 1226B.

UTC time (s)	Date (GMT)	Time (GMT)	TPC temperature				Conductivity probe		TPC pressure		TPC depth (m)
			(bits)	( $\Omega$ )	(K)	( $^{\circ}$ C)	1 (bits)	2 (bits)	(bits)	(psig)	
1014184800	2/20/02	6:00:00	2949	12376.0664165224	293.3523380577	20.3523380577	90	3829	0	0.0	0.0
1014184801	2/20/02	6:00:01	2949	12376.0664165224	293.3523380577	20.3523380577	3782	995	0	0.0	0.0
1014184802	2/20/02	6:00:02	2948	12383.6293881977	293.3387984206	20.3387984206	88	988	0	0.0	0.0
1014184803	2/20/02	6:00:03	2948	12383.6293881977	293.3387984206	20.3387984206	3786	3821	0	0.0	0.0
1014184804	2/20/02	6:00:04	2949	12376.0664165224	293.3523380577	20.3523380577	93	989	0	0.0	0.0
1014184805	2/20/02	6:00:05	2949	12376.0664165224	293.3523380577	20.3523380577	3784	3829	0	0.0	0.0
1014184806	2/20/02	6:00:06	2949	12376.0664165224	293.3523380577	20.3523380577	3804	980	0	0.0	0.0
1014184807	2/20/02	6:00:07	2948	12383.6293881977	293.3387984206	20.3387984206	87	986	0	0.0	0.0
1014184808	2/20/02	6:00:08	2948	12383.6293881977	293.3387984206	20.3387984206	71	994	0	0.0	0.0
1014184809	2/20/02	6:00:09	2949	12376.0664165224	293.3523380577	20.3523380577	80	1009	0	0.0	0.0
1014184810	2/20/02	6:00:10	2948	12383.6293881977	293.3387984206	20.3387984206	88	1017	0	0.0	0.0
1014184811	2/20/02	6:00:11	2948	12383.6293881977	293.3387984206	20.3387984206	3754	1008	0	0.0	0.0
1014184812	2/20/02	6:00:12	2948	12383.6293881977	293.3387984206	20.3387984206	118	1012	0	0.0	0.0
1014184813	2/20/02	6:00:13	2948	12383.6293881977	293.3387984206	20.3387984206	3816	3851	0	0.0	0.0
1014184814	2/20/02	6:00:14	2948	12383.6293881977	293.3387984206	20.3387984206	121	1010	0	0.0	0.0
1014184815	2/20/02	6:00:15	2949	12376.0664165224	293.3523380577	20.3523380577	3814	3841	0	0.0	0.0
1014184816	2/20/02	6:00:16	2949	12376.0664165224	293.3523380577	20.3523380577	126	3843	0	0.0	0.0
1014184817	2/20/02	6:00:17	2949	12376.0664165224	293.3523380577	20.3523380577	3808	3833	0	0.0	0.0
1014184818	2/20/02	6:00:18	2949	12376.0664165224	293.3523380577	20.3523380577	3824	3836	0	0.0	0.0
1014184819	2/20/02	6:00:19	2949	12376.0664165224	293.3523380577	20.3523380577	3814	986	0	0.0	0.0
1014184820	2/20/02	6:00:20	2949	12376.0664165224	293.3523380577	20.3523380577	95	992	0	0.0	0.0
1014184821	2/20/02	6:00:21	2949	12376.0664165224	293.3523380577	20.3523380577	78	1000	0	0.0	0.0
1014184822	2/20/02	6:00:22	2948	12383.6293881977	293.3387984206	20.3387984206	87	3838	0	0.0	0.0
1014184823	2/20/02	6:00:23	2949	12376.0664165224	293.3523380577	20.3523380577	3805	999	0	0.0	0.0
1014184824	2/20/02	6:00:24	2948	12383.6293881977	293.3387984206	20.3387984206	3826	995	0	0.0	0.0
1014184825	2/20/02	6:00:25	2948	12383.6293881977	293.3387984206	20.3387984206	3825	3837	0	0.0	0.0
1014184826	2/20/02	6:00:26	2948	12383.6293881977	293.3387984206	20.3387984206	104	3838	0	0.0	0.0
1014184827	2/20/02	6:00:27	2948	12383.6293881977	293.3387984206	20.3387984206	227	3829	0	0.0	0.0
1014184828	2/20/02	6:00:28	2948	12383.6293881977	293.3387984206	20.3387984206	3792	3822	0	0.0	0.0
1014184829	2/20/02	6:00:29	2948	12383.6293881977	293.3387984206	20.3387984206	3808	3824	0	0.0	0.0
1014184830	2/20/02	6:00:30	2948	12383.6293881977	293.3387984206	20.3387984206	3799	984	0	0.0	0.0
1014184831	2/20/02	6:00:31	2948	12383.6293881977	293.3387984206	20.3387984206	81	3824	0	0.0	0.0
1014184832	2/20/02	6:00:32	2948	12383.6293881977	293.3387984206	20.3387984206	3772	3818	0	0.0	0.0
1014184833	2/20/02	6:00:33	2948	12383.6293881977	293.3387984206	20.3387984206	3788	970	0	0.0	0.0
1014184834	2/20/02	6:00:34	2948	12383.6293881977	293.3387984206	20.3387984206	72	1178	0	0.0	0.0
1014184835	2/20/02	6:00:35	2948	12383.6293881977	293.3387984206	20.3387984206	57	3818	0	0.0	0.0
1014184836	2/20/02	6:00:36	2948	12383.6293881977	293.3387984206	20.3387984206	62	3827	0	0.0	0.0
1014184837	2/20/02	6:00:37	2948	12383.6293881977	293.3387984206	20.3387984206	65	995	0	0.0	0.0
1014184838	2/20/02	6:00:38	2948	12383.6293881977	293.3387984206	20.3387984206	3782	3817	0	0.0	0.0
1014184839	2/20/02	6:00:39	2948	12383.6293881977	293.3387984206	20.3387984206	92	3820	0	0.0	0.0
1014184840	2/20/02	6:00:40	2948	12383.6293881977	293.3387984206	20.3387984206	3777	978	0	0.0	0.0
1014184841	2/20/02	6:00:41	2948	12383.6293881977	293.3387984206	20.3387984206	85	3822	0	0.0	0.0
1014184842	2/20/02	6:00:42	2947	12391.1969438878	293.3252599362	20.3252599362	3777	987	0	0.0	0.0
1014184843	2/20/02	6:00:43	2947	12391.1969438878	293.3252599362	20.3252599362	86	3827	0	0.0	0.0
1014184844	2/20/02	6:00:44	2947	12391.1969438878	293.3252599362	20.3252599362	3777	987	0	0.0	0.0
1014184845	2/20/02	6:00:45	2947	12391.1969438878	293.3252599362	20.3252599362	86	3817	0	0.0	0.0

Notes: UTC = universal time coordinated, GMT = Greenwich mean time, TPC = temperature, pressure, and conductivity tool. Only a portion of this table appears here. The complete table is available in [ASCI](#).

Table T2. Raw and derived data, Hole 1226E.

UTC time (s)	Date (GMT)	Time (GMT)	TPC temperature				Conductivity probe		TPC pressure		TPC depth (m)
			(bits)	( $\Omega$ )	(K)	( $^{\circ}$ C)	1 (bits)	2 (bits)	(bits)	(psig)	
1014503294	2/22/98	22:28:14	2952	12353.4049448492	293.3929639467	20.3929639467	0	3684	0	0.0	0.0
1014503295	2/22/98	22:28:15	2952	12353.4049448492	293.3929639467	20.3929639467	3594	849	0	0.0	0.0
1014503296	2/22/98	22:28:16	2952	12353.4049448492	293.3929639467	20.3929639467	3611	849	0	0.0	0.0
1014503297	2/22/98	22:28:17	2952	12353.4049448492	293.3929639467	20.3929639467	3610	849	0	0.0	0.0
1014503298	2/22/98	22:28:18	2952	12353.4049448492	293.3929639467	20.3929639467	0	850	0	0.0	0.0
1014503299	2/22/98	22:28:19	2952	12353.4049448492	293.3929639467	20.3929639467	0	844	0	0.0	0.0
1014503300	2/22/98	22:28:20	2952	12353.4049448492	293.3929639467	20.3929639467	3575	842	0	0.0	0.0
1014503301	2/22/98	22:28:21	2952	12353.4049448492	293.3929639467	20.3929639467	3613	841	0	0.0	0.0
1014503302	2/22/98	22:28:22	2951	12360.9542009077	293.3794208146	20.3794208146	3610	3676	0	0.0	0.0
1014503303	2/22/98	22:28:23	2952	12353.4049448492	293.3929639467	20.3929639467	3608	3685	0	0.0	0.0
1014503304	2/22/98	22:28:24	2952	12353.4049448492	293.3929639467	20.3929639467	3606	849	0	0.0	0.0
1014503305	2/22/98	22:28:25	2952	12353.4049448492	293.3929639467	20.3929639467	0	2315	0	0.0	0.0
1014503306	2/22/98	22:28:26	2951	12360.9542009077	293.3794208146	20.3794208146	0	850	0	0.0	0.0
1014503307	2/22/98	22:28:27	2952	12353.4049448492	293.3929639467	20.3929639467	3591	851	0	0.0	0.0
1014503308	2/22/98	22:28:28	2952	12353.4049448492	293.3929639467	20.3929639467	0	3678	0	0.0	0.0
1014503309	2/22/98	22:28:29	2951	12360.9542009077	293.3794208146	20.3794208146	3585	849	0	0.0	0.0
1014503310	2/22/98	22:28:30	2952	12353.4049448492	293.3929639467	20.3929639467	0	3657	0	0.0	0.0
1014503311	2/22/98	22:28:31	2951	12360.9542009077	293.3794208146	20.3794208146	3586	3676	0	0.0	0.0
1014503312	2/22/98	22:28:32	2951	12360.9542009077	293.3794208146	20.3794208146	0	3678	0	0.0	0.0
1014503313	2/22/98	22:28:33	2951	12360.9542009077	293.3794208146	20.3794208146	3584	849	0	0.0	0.0
1014503314	2/22/98	22:28:34	2951	12360.9542009077	293.3794208146	20.3794208146	0	843	0	0.0	0.0
1014503315	2/22/98	22:28:35	2951	12360.9542009077	293.3794208146	20.3794208146	0	3676	0	0.0	0.0
1014503316	2/22/98	22:28:36	2951	12360.9542009077	293.3794208146	20.3794208146	3590	840	0	0.0	0.0
1014503317	2/22/98	22:28:37	2951	12360.9542009077	293.3794208146	20.3794208146	3610	3672	0	0.0	0.0
1014503318	2/22/98	22:28:38	2951	12360.9542009077	293.3794208146	20.3794208146	3472	850	0	0.0	0.0
1014503319	2/22/98	22:28:39	2951	12360.9542009077	293.3794208146	20.3794208146	3611	3675	0	0.0	0.0
1014503320	2/22/98	22:28:40	2951	12360.9542009077	293.3794208146	20.3794208146	3609	3682	0	0.0	0.0
1014503321	2/22/98	22:28:41	2951	12360.9542009077	293.3794208146	20.3794208146	3610	3686	0	0.0	0.0
1014503322	2/22/98	22:28:42	2951	12360.9542009077	293.3794208146	20.3794208146	0	3677	0	0.0	0.0
1014503323	2/22/98	22:28:43	2951	12360.9542009077	293.3794208146	20.3794208146	2394	877	0	0.0	0.0
1014503324	2/22/98	22:28:44	2951	12360.9542009077	293.3794208146	20.3794208146	0	3726	0	0.0	0.0
1014503325	2/22/98	22:28:45	2951	12360.9542009077	293.3794208146	20.3794208146	3637	942	0	0.0	0.0
1014503326	2/22/98	22:28:46	2951	12360.9542009077	293.3794208146	20.3794208146	306	3818	0	0.0	0.0
1014503327	2/22/98	22:28:47	2951	12360.9542009077	293.3794208146	20.3794208146	65	3853	0	0.0	0.0
1014503328	2/22/98	22:28:48	2951	12360.9542009077	293.3794208146	20.3794208146	172	3861	0	0.0	0.0
1014503329	2/22/98	22:28:49	2951	12360.9542009077	293.3794208146	20.3794208146	3842	3890	0	0.0	0.0
1014503330	2/22/98	22:28:50	2952	12353.4049448492	293.3929639467	20.3929639467	3888	3894	0	0.0	0.0
1014503331	2/22/98	22:28:51	2951	12360.9542009077	293.3794208146	20.3794208146	3907	3916	0	0.0	0.0
1014503332	2/22/98	22:28:52	2951	12360.9542009077	293.3794208146	20.3794208146	206	1094	0	0.0	0.0
1014503333	2/22/98	22:28:53	2952	12353.4049448492	293.3929639467	20.3929639467	3898	3946	0	0.0	0.0
1014503334	2/22/98	22:28:54	2952	12353.4049448492	293.3929639467	20.3929639467	3973	1119	0	0.0	0.0
1014503335	2/22/98	22:28:55	2952	12353.4049448492	293.3929639467	20.3929639467	273	1152	0	0.0	0.0
1014503336	2/22/98	22:28:56	2952	12353.4049448492	293.3929639467	20.3929639467	291	1159	0	0.0	0.0
1014503337	2/22/98	22:28:57	2952	12353.4049448492	293.3929639467	20.3929639467	4093	1168	0	0.0	0.0
1014503338	2/22/98	22:28:58	2951	12360.9542009077	293.3794208146	20.3794208146	4095	1191	0	0.0	0.0

Notes: UTC = universal time coordinated, GMT = Greenwich mean time, TPC = temperature, pressure, and conductivity tool. Only a portion of this table appears here. The complete table is available in [ASCII](#).



**Table T3.** Depths at which headspace gas disappeared and reappeared at Site 1226.

Core	Depth to top of core (mbsl)	Depth of disappearance of gas headspace (mbsl)	Depth of reappearance of gas headspace (mbsl)	Depth difference (m)
201-1226B-				
5H	3329.9	No loss of headspace	No loss of headspace	
6H	3339.4	2730	2570	160
7H	3348.9	No loss of headspace	No loss of headspace	
8H	3358.4	2900	2730	170
9H	3367.9	2700	2480	220
10H	3377.4	No loss of headspace	No loss of headspace	
201-1226E-				
5H	3332.5	3120	1850	1270
6H	3342.0	2000	1900	100
7H	3351.5	250	480	-230
8H	3361.0	No loss of headspace	No loss of headspace	
9H	3370.5	70	20	50
10H	3380.0	No loss of headspace	No loss of headspace	
11H	3389.5	280	400	-120
12H	3399.0	2250	1360	890